Pressure Effect on the Structural Transition and Suppression of the High-Spin State in the Triple-Layer T'-$La_4Ni_3O_8$

J.-G. Cheng,[1] J.-S. Zhou,[1,*] J. B. Goodenough,[1] H. D. Zhou,[2] K. Matsubayashi,[3] Y. Uwatoko,[3] P. P. Kong,[4] C. Q. Jin,[4] W. G. Yang,[5] and G. Y. Shen[5]

[1]*Materials Science and Engineering Program/Mechanical Engineering, University of Texas at Austin, Austin, Texas 78712, USA*

[2]*NHMFL, Florida State University, Tallahassee, Florida 32306, USA*

[3]*Institute for Solid State Physics, University of Tokyo, Kashiwa 277-8581, Japan*

[4]*Institute of Physics, Chinese Academy of Sciences, Beijing 100190, China*

[5]*High Pressure Synergetic Consortium (HPSynC) and High Pressure Collaborative Access Team (HPCAT), Geophysical Laboratory, Carnegie Institution of Washington, Argonne, Illinois 60439, USA*

(Received 2 February 2012; published 8 June 2012)

We report a comprehensive high-pressure study on the triple-layer T'-$La_4Ni_3O_8$ with a suite of experimental probes, including structure determination, magnetic, and transport properties up to 50 GPa. Consistent with a recent *ab inito* calculation, application of hydrostatic pressure suppresses an insulator-metal spin-state transition at $P_c \approx 6$ GPa. However, a low-spin metallic phase does not emerge after the high-spin state is suppressed to the lowest temperature. For $P > 20$ GPa, the ambient T' structure transforms gradually to a $T^{\dagger}$-type structure, which involves a structural reconstruction from fluorite La-O_2-La blocks under low pressures to rock-salt LaO-LaO blocks under high pressures. Absence of the metallic phase under pressure has been discussed in terms of local displacements of O^{2-} ions in the fluorite block under pressure before a global $T^{\dagger}$ phase is established.

DOI: 10.1103/PhysRevLett.108.236403 PACS numbers: 71.30.+h, 61.50.Ks, 61.66.Fn, 81.40.Vw

The T'-type triple-layer $R_4Ni_3O_8$ (R = La, Pr, and Nd) can be obtained via a low-temperature reduction of the corresponding T- or O-type Ruddlesden-Popper phase $R_4Ni_3O_{10}$ [1]. As shown in Fig. 1, the transformation from triple-layer T- or O-$La_4Ni_3O_{10}$ to T'-$La_4Ni_3O_8$ involves: (1) a removal of two apical oxygen atoms of the inner NiO_6 octahedra and (2) a rearrangement of the rock-salt LaO-LaO layer to a fluorite La-O_2-La layer via the displacement of one apical oxygen atom of the outer NiO_6 octahedra. The crystal structure of T'-$La_4Ni_3O_8$ can be described by stacking alternately the (La-O_2-La) fluorite-type layers with NiO_2 infinite-layer blocks along the c axis of a tetragonal unit cell with the I4/mmm space group. The three successive NiO_2 infinite planes are separated by a single La^{3+}-ion layer with an interplane distance of 3.25 Å, much smaller than the intraplane Ni-Ni separation of 3.93 Å. In a simple ionic picture, the average Ni valence is +1.33 and the ratio of Ni^{1+}/Ni^{2+} ($3d^9/3d^8$) is 2:1. Interest in the T'-type nickelate with mixed-valence Ni^{1+}/Ni^{2+} ions stabilized in a square-coplanar coordination has been revived since it has been argued theoretically [2] to be the direct analog of the high-T_c cuprates with Cu^{2+}/Cu^{3+}; the compound also shows quantum confinement and a temperature-driven spin-state transition at low temperatures [3–6].

T'-$La_4Ni_3O_8$ undergoes an abrupt phase transition at $T_t = 105$ K as indicated by measurements of transport and magnetic properties as well as the specific heat [3]. However, neutron diffraction failed to confirm any long-range spin ordering below T_t [3]. Although an NMR study [5] revealed Fermi liquid behavior above 250 K and significant critical spin fluctuations at $T > T_t$, a semiconductive $\rho(T)$ has been observed at $T > T_t$. This contradiction could be due to the poorly compacted polycrystalline sample used for the conductivity study.

Nickel with square coplanar coordination in the layered T'-$La_4Ni_3O_8$ can have either a low-spin (LS) configuration $(d^{\uparrow\downarrow}_{3z^2-r^2})^2(d^{\uparrow}_{x^2-y^2})^{0.67}$ or a high-spin (HS) configuration

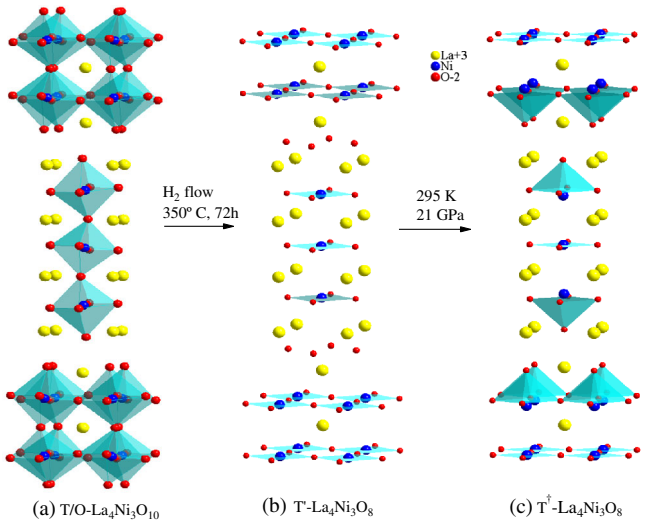

FIG. 1 (color online). Crystal structures of the Ruddlesden-Popper phase $La_4Ni_3O_{10}$, T' phase, and $T^{\dagger}$ phase of $La_4Ni_3O_8$.

$(d^{\uparrow}_{3z^2-r^2})^1(d^{\uparrow}_{x^2-y^2})^1(d^{\downarrow}_{3z^2-r^2})^{0.67}$. A density-function-theory calculation predicted a metallic LS phase and an antiferromagnetic-insulator HS phase [7]. Based on the electronic configuration, the LS phase should have a shorter Ni-O bond length within a NiO_2 layer than that in the HS phase. It has been argued [8] that the transition at T_t is actually due to a HS-LS spin-state transition. However, no published data are available to confirm the argument. Based on their calculation, Pardo and Pickett [7] have shown that the cell volume in the LS phase should be smaller than that in the HS phase, so that high pressure prefers the LS phase. They have further predicted that the HS phase would be suppressed and therefore the LS metallic phase should persist to the lowest temperature under $P \approx 5$ GPa. A direct comparison between the LS metallic phase in the T'-$La_4Ni_3O_8$ and high-T_c cuprates at low temperatures makes the high-pressure experiment extremely interesting. In this Letter, we report a comprehensive high-pressure study on the T'-$La_4Ni_3O_8$.

Polycrystalline T'-$La_4Ni_3O_8$ samples were prepared by a low-temperature reduction of a $La_4Ni_3O_{10-\delta}$ precursor obtained with a sol-gel method [9]. The preparation of pellets with a regular die gave porous bulk samples after the final step of hydrogen reduction. We have applied the cold-press technique to make pellets before the hydrogen reduction. Although pellets were shattered into small clusters after the hydrogen reduction, a highly densified cluster of about 1 mm in dimension was sufficient for us to measure transport properties. Details about the sample's preparation and characterizations at ambient pressure are given in the Supplemental Material [10]. The *in situ* HP synchrotron angle-dispersive x-ray diffraction (SXRD) at room temperature (RT) was performed at the 16BM-D station of the Advanced Photon Source in the Argonne National Laboratory with a wavelength 0.4247 Å by using a diamond anvil cell (DAC) with 400 μm cullet diamonds. Silicon oil was used as the pressure-transmitting medium. The ruby-fluorescence method was used to monitor the pressure. The diffraction patterns were collected by using a Mar345 image-plate detector. The intensity versus 2θ patterns were obtained with FIT2D software. Resistivity $\rho(T)$ in the temperature range 5–300 K was measured at different pressures up to 50 GPa. The $\rho(T)$ measurement under pressures up to 2 GPa were carried out at the University of Texas at Austin (UTA) with a self-clamped piston-cylinder Be-Cu device (PCD). Daphne 7373 was used as the pressure-transmitting medium; the pressure inside the Teflon cell was monitored by a manganin manometer. The measurements of $\rho(T)$ up to 8 GPa have been done at ISSP, University of Tokyo with a cubic multianvil device (CMD) filled with liquid-pressure medium. The measurements of $\rho(T)$ up to 50 GPa were performed at IOP, Beijing, China with a two-probe method in a DAC. MgO fine powder was used as the insulating layer on a stainless steel (T301) gasket and *h*-BN was used as the solid pressure-transmitting medium. The pressure applied at RT was monitored by the ruby-fluorescence method. The magnetization measurements under pressure were performed with a homemade piston-cylinder device fit to a commercial SQUID magnetometer (Quantum Design). The sample together with a small piece of Pb as the pressure manometer was sealed in a Teflon cell filled with Daphne 7373.

Figure 2 shows the temperature dependences of the magnetic and transport properties and lattice parameters of the T'-$La_4Ni_3O_8$ at ambient pressure. $M(T)$ in Fig. 2(a) is identical to that reported by Poltavets *et al.* [3] However, the overall resistivity of our sample is lower by one order than that reported by Poltavets *et al.* [3] due to the highly densified sample in our study. The sharpness of the transition at T_t is also improved and an interesting curvature of $\rho(T)$ appears at $T \sim 180$ K that could be related to the onset of critical spin fluctuations picked up by the NMR measurement [5]. The thermoelectric power $S(T)$ in Fig. 2(c) is new. Since the thermoelectric-power measurement reflects the intrinsic property even in polycrystalline samples, a small thermoelectric power and the temperature dependence fitting the Mott diffusive formula indeed confirm a metallic phase at $T > T_t$. An abrupt increase of $|S|$ on cooling through T_t indicates unambiguously a gap opening at the Fermi energy in the phase at $T < T_t$.

More important information about the nature of the transition at T_t can be extracted from the temperature dependences of the lattice parameters. A clear jump of the a axis and a drop of the c axis in Figs. 2(d) and 2(e) on cooling through T_t are consistent with the scenario of the LS-HS transition at T_t. Most importantly, the cell volume of the phase at $T < T_t$ is larger than that

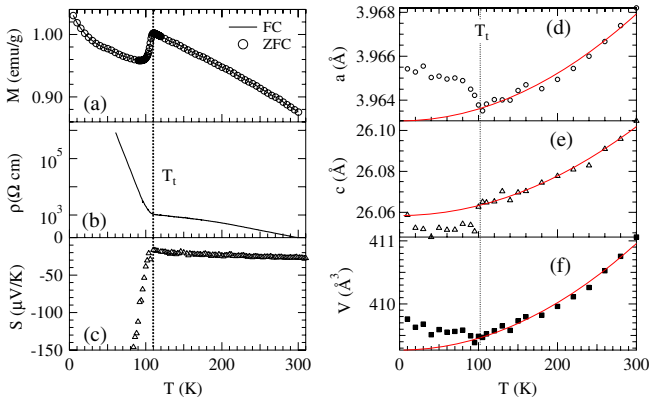

FIG. 2 (color online). Temperature dependence of (a) magnetization with $H = 5$ T; the zero-field-cool and field-cool curves overlap (b) resistivity, (c) thermoelectric power, and (d)–(f) lattice parameters for T'-$La_4Ni_3O_8$. Error bars in these plots are smaller than symbols. Lattice parameters at $T > T_t$ are fit with a polynomial formula.

extrapolated from the phase at $T > T_t$. This observation has actually motivated this high-pressure study before we became aware of the calculation by Pardo and Pickett [7].

We now focus on the central issue of how T'-$La_4Ni_3O_8$ behaves under high pressure. Figure 3 displays the temperature dependence of resistivity under high pressure, which was measured with two experimental setups. High pressure lowers the resistivity over the entire temperature range, especially in the HS phase at $T < T_t$. The measurements with the PCD allow us to monitor in great detail how T_t is suppressed under pressure. However, a pressure $P \sim 2$ GPa, the upper limit for the device, is insufficient to reduce T_t to the lowest temperature. In a separate experiment, the same sample was loaded in the CMD; $\rho(T)$ at $P = 3$ GPa measured with the CMD is similar to that at $P = 2$ GPa obtained with the PCD. For $P \geq 2$ GPa, the transition at T_t becomes broad and difficult to define in the plot of Fig. 3(b). We have integrated the transport data under pressure collected from two different setups into a plot of $\ln\rho$ versus $T^{-1/4}$ in Fig. 3(c). It is clear from this plot that the low-temperature phase remains an insulator phase after T_t is suppressed. The range showing a linear dependence in this plot can be described by the variable-range-hopping conductivity. At $P = 3$ GPa, the overall curve consists of three nearly linear parts; slope changes can be seen unambiguously at T_t and T_0. These features remain nearly unchanged up to 6 GPa except that the linear part at $T > T_t$ extends to higher temperatures. At 8 GPa, the feature for defining T_t totally disappears. We have also measured the resistivity with a DAC up to 50 GPa (see the Supplemental Material [10] for the detailed results). The high-pressure phase remains an insulator from 50 K to room temperature.

The change of T_t under pressure has also been confirmed by the magnetization measurement shown in Fig. 4(a). The transition temperature T_t can be well defined in the pressure range to 1 GPa. The T_t versus P from this measurement is plotted in Fig. 4(b) together with the data from measurements of the transport property. The pressure dependences of T_t obtained from both measurements are highly consistent; T_t decreases linearly under pressure up to 2 GPa with a slope $dT_t/dP = 17.2$ K/GPa. Whereas the feature at T_t becomes blurred, T_t becomes essentially pressure-independent in the interval $2 \leq P \leq 6$ GPa, where T_t disappears. The broad transition at T_0 in the plot of $\ln\rho$ versus $T^{-1/4}$ in Fig. 3(c) is more likely related to the onset of critical spin fluctuations detected by the NMR measurement. Applying high pressure ends up with a variable-range-hopping insulator phase, which is not only sharply contradictory to the prediction by Pardo and Pickett [7], but also inconsistent with the fact that pressure stabilizes the LS phase at lower pressures. In order to understand what really happens under pressure, we turn to the structural study under high pressure.

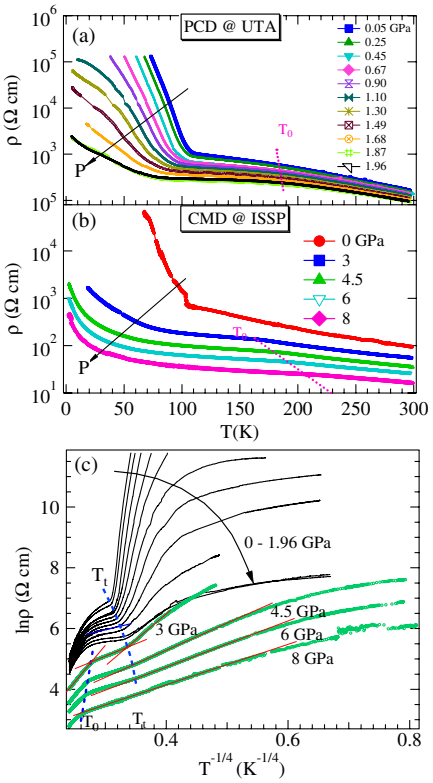

FIG. 3 (color online). Temperature dependence of resistivity for T'-$La_4Ni_3O_8$ under different pressures. Solid lines in Fig. 3(c) are to guide the eyes. Curves presented as thick lines were obtained with a cubic multianvil device. See the Supplemental Material [10] for detailed clarification.

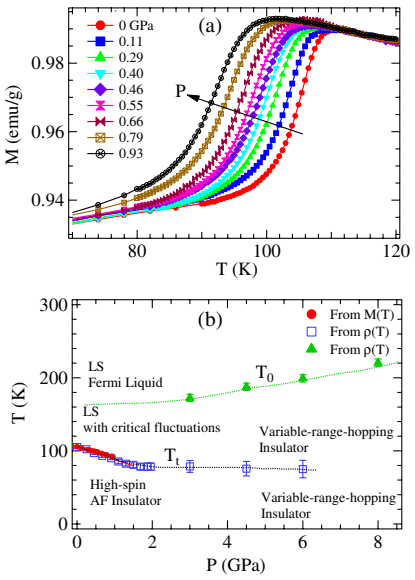

FIG. 4 (color online). (a) Temperature dependence of the magnetization under different pressures; (b) the temperature-pressure phase diagram of T'-$La_4Ni_3O_8$.

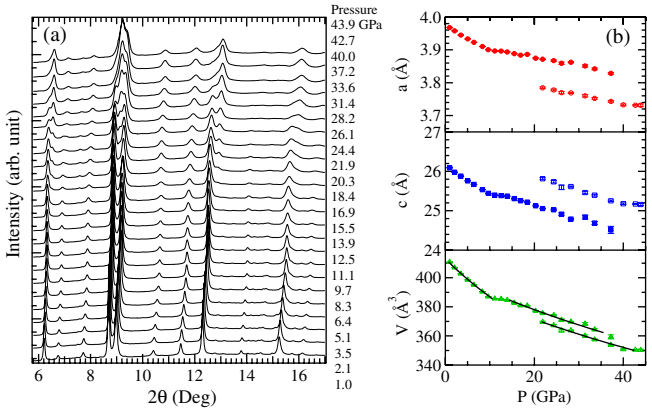

FIG. 5 (color online). (a) SXRD patterns at room temperature under different pressures; (b) Lattice parameters as a function of pressure; lines inside the $V(P)$ curve are results of the curve fitting to the Birch-Murnaghan equation.

Figure 5 shows SXRD patterns under different pressures at room temperature. The T' structure of $La_4Ni_3O_8$ remains stable up to $P \approx 21$ GPa. For $P > 21$ GPa, shoulders develop for peaks at $2\theta = 6.5°$ and 12.5°. The two phases coexist in the pressure range 21–40 GPa and the SXRD pattern shows single phase again for $P > 40$ GPa. An initial trial indexing indicates that the high-pressure phase has a shorter a axis and a longer c axis than that in the T' structure. The structural change from T-$La_4Ni_3O_{10}$ to T'-$La_4Ni_3O_{10}$ in Fig. 1 involves removing the apical oxygen inside the triple Ni-O layers and displacing the apical oxygen in the rock-salt structure to the oxygen-only plane in the fluorite La-O_2-La block. The strong Coulombic force in the oxygen-only layer stretches the ab plane in the T' structure. This structural transition is characterized by enlarging the a axis and reducing the c axis. The same changes in lattice parameters can also be found in the structural transition from T- or O-R_2CuO_4 to T'-R_2CuO_4 [11,12] Since there is no way for the sample in the high-pressure chamber to gain extra oxygen, the high-pressure phase of $La_4Ni_3O_8$ at $P > 20$ GPa is most likely to have the T structure without the apical oxygen in the inner layer; the model of this $T^\dagger$ structure is displayed in Fig. 1(c). This conjecture makes sense since high pressure prefers the T or O structure relative to the T' structure as observed in $La_{2-x}Nd_xCuO_4$ [13]. The profile of the SXRD pattern of the high-pressure phase can be indeed refined reasonably well based on the structural model in Fig. 1(c). The fitted SXRD pattern and fitting results can be found in the Supplemental Material [10]. Lattice parameters as a function of pressure in Fig. 5(b) have been obtained from the full-profile fitting to the SXRD patterns in three pressure ranges corresponding to T', $T' + T^\dagger$, and $T^\dagger$ structures. Both a and c reduce monotonically under pressure. The T' phase is relatively soft at low pressures with a bulk modulus $B_0 = 134$ GPa, which is far less than most perovskite oxides and below the estimated value $B_0 = 180$ GPa used by Pardo and Pickett in their calculation. It is interesting that the slope of V versus P curve changes at $P \geq 10$ GPa. The "hard" T' phase with a bulk modulus $B_0 = 258$ GPa extends into the two-phase range before disappearing at $P \approx 39$ GPa. The $T^\dagger$ phase has a relatively smaller cell volume than the T' phase. The bulk modulus $B_0 = 260$ GPa of the $T^\dagger$ phase is unusually high. The T' to $T^\dagger$ phase transition is reversible and clearly a hysteresis loop has been observed on increasing and releasing pressure; see the Supplemental Material [10] for the detailed results.

The high-pressure structural study by SXRD shows the global structure change under pressure. However, isolated oxygen displacements from the oxygen-only layer in the fluorite block to the apical site for Ni in the outer NiO_2 layer may occur in the global T' structure under a pressure that is much lower than P_c for triggering the T' to $T^\dagger$ phase transition. The presence of apical oxygen would raise the antibonding d_{z^2} band relative to the occupied $d_{x^2-y^2}$ band so as to stabilize the HS state. These isolated HS Ni ions also perturb the long-range periodicity of the lattice, which leads to the variable hopping conductivity in Fig. 3 under higher pressures. As a matter of fact, the observation of a pressure-independent T_t for $2 \leq P \leq 6$ GPa in the phase diagram of Fig. 4 reflects precisely a two-phase coexistence in this pressure range although the SXRD is not sensitive enough to detect the second phase. Similarly, isolated apical oxygen in the n-type $Nd_{2-x}Ce_xCuO_4$ with the T' structure suppresses superconductivity [14].

As indicated in the temperature dependence of lattice parameters of Fig. 2, the slightly larger cell volume of the HS phase makes it unstable relative to the LS phase under high pressure. However, pressure induces isolated oxygen displacements in the T' structure before it induces a global structural transition at $P > 21$ GPa. The HS state is stabilized at isolated Ni sites with the oxygen displacements. This pressure-induced structural change has been missed in the calculation that predicts the overall stabilization of the LS phase under high pressure [7].

In conclusion, the metal-insulator transition at 105 K in the T'-$La_4Ni_3O_8$ is associated with significant changes of lattice parameters. These changes are consistent with the model of a temperature-driven high-spin to low-spin transition at T_t. A jump of cell volume on cooling through T_t suggests that the LS phase would be stabilized to the lowest temperature under a sufficiently high pressure. While T_t is indeed suppressed under pressure as indicated by the measurements of transport and magnetic properties under pressure, the LS phase has not been observed to be metallic under high pressure. The high-pressure structural study reveals that a new $T^\dagger$ structure is stabilized under $P > 21$ GPa. The presence of isolated Ni sites with apical oxygen in the T' structure leads to a variable-range-hopping conductivity in the LS phase in which T_t is suppressed under pressure.

This work was supported by the NSF (DMR0904282, MIRT DMR1122603, and DMR0654118), the Robert A.

Welch Foundation (Grant No. F-1066), the State of Florida, the NSF and MOST of China, and Grant-in-Aid for Scientific Research in Japan. HPSynC and HPCAT are supported by CIW, CDAC, UNLV, and LLNL through funding from DOE-NNSA, DOE-BES, and NSF.

*jszhou@mail.utexas.edu

[1] Ph. Lacorre, J. Solid State Chem. **97**, 495 (1992).
[2] V. I. Anisimov, D. Bukhvalov, and T. M. Rice, Phys. Rev. B **59**, 7901 (1999).
[3] V. V. Poltavets, K. A. Lokshin, A. H. Nevidomskyy, M. Croft, T. A. Tyson, J. Hadermann, G. Van Tendeloo, T. Egami, G. Kotliar, N. ApRoberts-Warren, A. P. Dioguardi, N. J. Curro, and M. Greenblatt, Phys. Rev. Lett. **104**, 206403 (2010).
[4] V. Pardo and W. E. Pickett, Phys. Rev. Lett. **105**, 266402 (2010).
[5] N. ApRoberts-Warren, A. P. Dioguardi, V. V. Poltavets, M. Greenblatt, P. Klavins, and N. J. Curro, Phys. Rev. B **83**, 014402 (2011).
[6] S. Sarkar, I. Dasgupta, M. Greenblatt, and T. Saha-Dasgupta, Phys. Rev. B **84**, 180411(R) (2011).
[7] V. Pardo and W. E. Pickett, Phys. Rev. B **85**, 045111 (2012).
[8] K. Lokshin and T. Egami, "Structure and Electronic Properties of the La_4-Ni_3-O_8," http://meetings.aps.org/Meeting/MAR11/Event/141968.
[9] V. V. Poltavets, K. A. Lokshin, T. Egami, and M. Greenblatt, Mater. Res. Bull. **41**, 955 (2006).
[10] See Supplemental Material at http://link.aps.org/supplemental/10.1103/PhysRevLett.108.236403 for the sample's preparation, characterization, and the result of Rietveld refinement of XRD, the transport property up to 50 GPa, and results of SXRD in a DAC with neon as the pressure medium.
[11] J. F. Bringley, S. S. Trail, and B. A. Scott, J. Solid State Chem. **86**, 310 (1990).
[12] A. Manthiram and J. B. Goodenough, J. Solid State Chem. **92**, 231 (1991).
[13] H. Wilhelm, C. Cros, F. Arrouy, and G. Demazeau, J. Solid State Chem. **126**, 88 (1996).
[14] J. S. Higgins, Y. Dagan, M. C. Barr, B. D. Weaver, and R. L. Greene, Phys. Rev. B **73**, 104510 (2006).